

Ground States of the Triangular Ising Model with Two- and Three-Spin Interactions

U. Brandt and J. Stolze

Institut für Physik, Universität Dortmund, Federal Republic of Germany

Received May 30, 1986

The possible ground state spin configurations of an Ising model on a plane triangular lattice are investigated. The model incorporates competing interactions between spins at nearest and next-nearest neighbour sites as well as a coupling between three spins at the vertices of a nearest-neighbour triangle, and an external magnetic field. Models of this type are frequently used to describe the structures of adsorbate layers on hexagonal substrates. The analysis is based on linear inequalities involving the magnetization, two- and three-spin correlations, and on simple convexity arguments. Part of the inequalities needed are proved with the aid of a computer. For vanishing three-spin coupling the results of earlier studies are confirmed; in addition, the resulting seven topologically distinct structures are shown to be unique. Two of these structures are energetically degenerate; the degeneracy cannot be lifted by any further two-spin interaction. For nonzero three-spin coupling only an "almost complete" solution is given, involving four additional spin configurations. The "ground state phase diagrams" are discussed.

I. Introduction

The Ising model on a triangular lattice has attracted the interest of physicists for two main reasons. From the point of view of theoretical statistical mechanics it has provided an early example [1, 2] of a system exhibiting macroscopic ground state degeneracy (violation of Nernst's theorem) due to what is nowadays called "frustration". In the field of solid state physics, on the other hand, the lattice gas version of this system has been used to describe the behaviour of submonolayers of adsorbate particles on substrates of hexagonal symmetry, e.g. the basal planes of graphite (cf. e.g. [3, 4]), and of intercalant layers in graphite intercalation compounds [5].

In the context of adsorbed layers, the influence of the crystalline substrate is reduced to the existence of a two-dimensional lattice of adsorption sites, and adsorbate-substrate interactions are summarized in a single binding energy. The interaction energy between adsorbate atoms is assumed to vanish except when atoms are adsorbed at near-neighbour sites. There remain only a few parameters describing the system. These parameters, however, are very difficult

to calculate due to the complex many-body nature of the original problem. Consequently, it is common practice to follow the alternative way of performing model calculations and comparing the results to experimental findings in order to estimate effective interaction parameters. Due to effects of competition between different forces, interactions of relatively short range suffice to create surprisingly complex structures. (Cf. e.g. the large unit cell ground state structures shown to exist in the square lattice [6-8] or even the infinite sequence of ground state structures reported for the honeycomb lattice [9], with pair interactions up to third neighbours in both cases.) One might thus try to achieve a rough phenomenological explanation of the rich variety [10] of ordered structures in adsorbate layers in terms of simple universal models.

Lattice gas (or Ising) models on a triangular lattice have been studied very often and by various methods. Without attempting to be complete, we mention some of the relevant references. In [1, 2], thermodynamic functions of the model with only nearest neighbour interactions (without external field) were calculated exactly, yielding a finite zero-

temperature entropy for antiferromagnetic coupling. Monte Carlo simulations were performed for the nearest-neighbour antiferromagnet in an external field [11] and also for the more complicated case involving an additional next-nearest neighbour interaction [12, 13]. This model (including interactions between nearest and next-nearest neighbours and an external magnetic field) was also treated by approximations of the molecular field type [14, 15] and (for zero field) by the interface method [16]; see [17] for the method. A model without next-nearest neighbour coupling, but with a three-spin interaction on a nearest-neighbour triangle was treated by real space renormalization [18]; the model with *only* three-spin interactions is exactly solvable [19]. If the nearest-neighbour interaction is antiferromagnetic (or repulsive, if we use the lattice gas language) and much stronger than the other interactions, as is the case for the adsorption of krypton and xenon on graphite, the lattice gas model may be mapped onto a three-state Potts model and treated by real space renormalization group methods [20] (see also [4] for further references on the use of Potts models in the context of rare gas submonolayers on graphite).

The rigorous determination of possible ground states of models with competing interactions is important as a complement to both mean field calculations (which become notoriously difficult in the presence of competing interactions) and Monte Carlo simulations (which become notoriously difficult at low temperatures). Furthermore a knowledge of possible ground states is helpful in guessing at the nature of phase transitions and in constructing reliable mean field approximations or renormalization group transformations.

It is to be expected that adding any further interaction (or an external field) to an antiferromagnetic nearest-neighbour interaction on the triangular lattice will destroy the infinite ground state degeneracy. However, the competition between nearest and next-nearest neighbour antiferromagnetic interactions might still lead to interesting effects, as each of these interactions leads to an infinitely degenerate ground state if taken by itself. (Note that the lattice may be decomposed into three triangular sublattices of next-nearest neighbour sites.) The first attempt at a complete determination of all ground state structures of a triangular model with interactions up to next nearest neighbours and an external field was made by Metcalf [21] with the help of Monte Carlo simulation. This author in fact found all possible ground state configurations except one. Kaburagi and Kanamori [22] used “geometrical inequalities” (to use their own terminology) to derive the complete set of ground states; their method is explained

(and applied to one dimensional and simple cubic systems) in [23]. The work of Kaburagi and Kanamori on the ground states of this and various other lattice gas models is reviewed in [24]. Kudo and Katsura [25] clearly pointed out the important role convexity plays in this method and treated three-dimensional hexagonal close-packed and honeycomb lattices (with interactions up to second and up to third neighbours, respectively). Tanaka and Uryû [26] introduced bond variables indicating the relative orientation of two adjacent spins and determined the ground state configurations of the triangular model with interactions up to second neighbours (but without magnetic field). In [27] Kaburagi and Kanamori extended the problem treated in [22] by adding an interaction between third neighbours and derived a large number of different structures. Some of these structures, however, could not be rigorously confirmed as ground states.

In the present paper, we study the ground state configurations of a model with an external magnetic field, two-spin interactions between nearest and next-nearest neighbours, and a three-spin interaction between sites at the vertices of a nearest-neighbour triangle. We use the method developed in [7] (which is closely related to the one used in [22], as improved in [25]), characterizing a spin configuration by the values of a few macroscopic parameters, namely the magnetization and some near-neighbour correlations, and deriving linear inequalities between these quantities. These inequalities define a multi-dimensional convex polyhedron (a simplex) in the space of macroscopic parameters, and the corners of the simplex correspond to ground state configurations.

In Sect. II we shall treat the case of vanishing three-spin interaction. We shall give very simple derivations for a set of inequalities which suffice to determine all possible ground state configurations for this case. Of course the resulting configurations (essentially there are seven different ones) are those already given in [22], however, we are able to show that these configurations are *uniquely* determined by the values of the macroscopic parameters mentioned above. We thus know that there are no degeneracies between structures of different superlattice cell sizes, except at “phase boundaries” in the “ground state phase diagram” and except for one region of coupling parameter space where two degenerate configurations coexist. The degeneracy between these configurations cannot be lifted by any two-spin interaction.

The case of nonvanishing three-spin coupling is treated in Sect. III; it turns out to be considerably more complicated than the problem treated in Sect.

II, so that we are not able to solve it completely. We prove some additional inequalities involving not only the magnetization and two-spin correlations, but also the three-spin correlation. Part of these inequalities are proved by a new method which we have developed and applied to an extended Hubbard model in the atomic limit [28]. This method mainly relies on the inspection of all possible spin configurations of a small cluster of lattice sites, which is most conveniently done by computer. Not all corners of the resulting simplex could be matched by spin configurations; in some cases we had to resort to Monte Carlo simulation to find ‘‘corner-like’’ spin configurations. The result of these efforts is a collection of four different (apart from symmetry operations) additional configurations, of which just one certainly is a new ground state. We know, however, that our solution is ‘‘almost complete’’ and we do not believe in the existence of additional ground states of spectacular shape or abundance.

In Sect. IV we shall discuss the ‘‘ground state phase diagrams’’ resulting from the ground state configurations derived in the two preceding sections.

II. The Model without Three-Spin Interactions and its Configurations

The model we study is defined by the Hamiltonian

$$H = -2B \sum_i \sigma_i - \frac{4}{3} J_1 \sum_{\langle NN \rangle} \sigma_i \sigma_j - \frac{4}{3} J_2 \sum_{\langle NNN \rangle} \sigma_i \sigma_j \\ =: -N(Bm + J_1 c_1 + J_2 c_2) \quad (\text{II.1})$$

with $\sigma_i = \pm 1/2$, magnetic field B and nearest- and next-nearest-neighbour couplings J_1 and J_2 , respectively ($J > 0$ corresponds to ferromagnetic coupling). The symbols $\langle NN \rangle$ and $\langle NNN \rangle$ denote summation over all distinct nearest- and next-nearest-neighbour pairs, respectively; the magnetization m is bounded by ± 1 , as are the correlations c_1 and c_2 . N is the number of lattice sites. Obviously this model may be related to a lattice-gas model in which every lattice site may be either occupied or empty. Introducing the lattice site occupation variables $n_i = 0, 1$ we may write down the following ‘‘grand canonical lattice gas Hamiltonian’’

$$H_{lg} - \mu N_{lg} \\ = -(\varepsilon + \mu) \sum_i n_i + F_1 \sum_{\langle NN \rangle} n_i n_j + F_2 \sum_{\langle NNN \rangle} n_i n_j \quad (\text{II.2})$$

where $N_{lg} = \sum_i n_i$, μ is the chemical potential and $F_{1,2}$ denote the interaction potentials between nearest and next-nearest neighbours, respectively. ε is the

binding energy of an adatom. Using the transformation $n_i = \sigma_i + 1/2$, we obtain the following correspondences between the parameters of (II.1) and (II.2):

$$-B \leftrightarrow \frac{3}{2}(F_1 + F_2) - \frac{1}{2}(\varepsilon + \mu), \\ -J_{1,2} \leftrightarrow \frac{3}{4}F_{1,2}. \quad (\text{II.3})$$

Our analysis (cf. [7, 28] of the ground state configurations of (II.1) is based on the fact that the set of all points (m, c_1, c_2) corresponding to different configurations of the system is convex in the thermodynamic limit, as Nm , Nc_1 , and Nc_2 are extensive quantities. In a first step we derive several linear inequalities between m , c_1 , and c_2 . These inequalities define a convex polyhedron (or simplex) in (m, c_1, c_2) -space, which contains all possible configurations. In a second step we construct configurations corresponding to the corners of the simplex, thus showing that *every* point of the simplex represents a possible configuration. (It is amusing to note that Wannier in his 1950 classic [1] already used an argument of this type to calculate the ground state energy of the triangular nearest neighbour antiferromagnet.) We finally determine the ground state configurations by noting that the energy is a linear function of m , c_1 and c_2 and thus assumes its extremal values at corners of the simplex.

Obviously every linear inequality between m , c_1 , and c_2 may be written in the form

$$b \leq a_1 m + a_2 c_1 + a_3 c_2. \quad (\text{II.4})$$

In Table 1 we give the coefficients b , a_1 , a_2 , a_3 of a set of inequalities which suffices to determine all ground state configurations.

Table 1. Coefficients of the inequalities of the form (II.4) which are used to determine the ground states of the Ising model (II.1)

Inequality No.	b	a_1	a_2	a_3
1	0	1	0	0
2	-1	-1	0	0
3	-1	0	-1	0
4	-1	0	0	-1
5	-1	0	3	0
6	-1	0	0	3
7	-1	-2	1	0
8	-1	-2	0	1
9	-1	-2	3/2	3/2
10	-1	-1	-3/2	3/2
11	-1	0	-2	1
12	-1	-2	5/2	1/2

Inequality 1 restricts our considerations to states of positive magnetization, inequalities 2–4 are trivial.

Inequality 5 is derived from

$$c_1 = \frac{1}{3N} \sum_i 4(\sigma_0 \sigma_1 + \sigma_0 \sigma_2 + \sigma_1 \sigma_2) \tag{II.5}$$

where the sum runs over all lattice sites and where the spin at site i is denoted by σ_0 and its nearest neighbours by $\sigma_1 \dots \sigma_6$ (in a definite sense of rotation). We now use the triangle inequality and the inequality

$$|n| \leq n^2 \quad (n \text{ integer}) \tag{II.6a}$$

to obtain

$$|c_1| \leq \frac{1}{3N} \sum_i 16(\sigma_0 \sigma_1 + \sigma_0 \sigma_2 + \sigma_1 \sigma_2)^2$$

from which the desired inequality follows. Inequalities 5 and 6 are equivalent, because each of the three interpenetrating next nearest neighbour sublattices is equivalent to the original lattice; the same holds true for inequalities 7 and 8. Inequality 7 is derived by starting from

$$m = \frac{2}{3N} \sum_i (\sigma_0 + \sigma_1 + \sigma_2) \tag{II.7}$$

and using the triangle inequality and

$$\left| \frac{2n+1}{2} \right| \leq \frac{3}{8} + \frac{1}{2} \left(\frac{2n+1}{2} \right)^2 \quad (n \text{ integer}). \tag{II.6b}$$

Inequalities 9, 10, and 12 are derived from

$$m = \frac{1}{2N} \sum_i (\sigma_0 + \sigma_1 + \sigma_3 + \sigma_5), \tag{II.8}$$

$$m = \frac{1}{N} \sum_i (-\sigma_0 + \sigma_1 + \sigma_3 + \sigma_5), \tag{II.9}$$

and

$$m = \frac{1}{2N} \sum_i (\sigma_0 + \sigma_1 + \sigma_2 + \sigma_3), \tag{II.10}$$

respectively, in an entirely analogous way. In order to derive inequality 11, we first decompose c_1 into three parts

$$c_1 = \frac{1}{3}(c_1(1, 3) + c_1(3, 5) + c_1(5, 1))$$

with

$$c_1(l, m) := \frac{1}{N} \sum_i 2(\sigma_0 \sigma_l + \sigma_0 \sigma_m)$$

and then proceed as above.

In Table 2 we list the corners of the simplex defined by the inequalities of Table 1.

Table 2. Ground states of the Ising model (II.1), as characterized by magnetization, two- and three-spin correlations, and superlattice unit cells

Corner No.	m	c_1	c_2	c_4	Structure
1	1	1	1	1	1×1
2	1/2	0	0	-1/2	2×2
3	1/3	-1/3	1	-1	$\sqrt{3} \times \sqrt{3}$
4a, b	1/3	1/9	-1/3	1/3, 1/9	$1 \times 3, 3 \times 3$
5	0	1/3	-1/3	0	1×4
6	0	-1/3	-1/3	0	1×2
7	0	-1/3	1	-	-
8	0	1	1	-	-

A little reflection reveals that the corners 7 and 8 are only artifacts of the restriction $m \geq 0$, i.e. each of them corresponds to a mixture of two configurations with $m = \pm |m|$, whereas 1, ..., 6 are "real corners". The entries in the columns named " c_4 " and "Structure" will be explained below.

The construction of spin configurations corresponding to corners 1, ..., 6 proceeds as follows. A corner is defined by the fact that (at least) three of the inequalities of Table 1 are simultaneously fulfilled as equalities. Retracing the derivations of the inequalities, we see that this puts constraints on the local configurations used in the derivations. For example, for inequality 7 (of Table 1) to be fulfilled as an equality, both the appropriate form of the triangle inequality and (II.6b) must be fulfilled as equalities. This is possible if $|\sigma_0 + \sigma_1 + \sigma_2| = 1/2$ (see (II.7)) for every nearest-neighbour triangle of the system and if $\sigma_0 + \sigma_1 + \sigma_2$ does not change sign. Thus configurations of positive magnetization fulfilling this inequality as an equality consist entirely of nearest neighbour triangles with exactly one down spin. This fixes the $\sqrt{3} \times \sqrt{3}$ configurations uniquely (up to symmetry operations, of course). Other examples are $c_2 = 1$, implying that the whole configuration is a combination of three fully polarized next nearest neighbour sublattices, and $c_1 = -1/3$, prohibiting the existence of any "fully polarized" nearest-neighbour triangle. Taking into account these constraints, we may build up the various configurations starting, say, from a single "up" spin. This procedure is unique except for corner no. 4, where two distinct configurations of equal energy exist (see Fig. 1). This degeneracy reflects the fact that there are essentially two ways to combine three next nearest neighbour sublattices in which every triangle contains exactly one down spin. In the last column of Table 2 we have characterized the various structures by their unit cells. We wish to stress once more that these

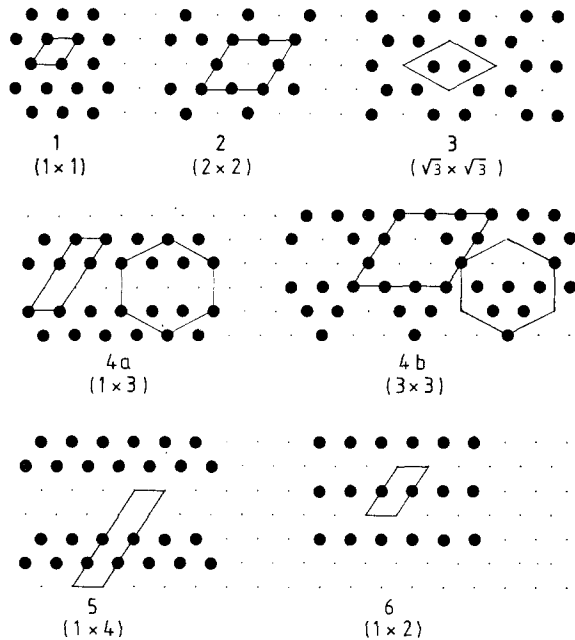


Fig. 1. Lattice configurations corresponding to the states listed in Table 2. Big dots represent “up” spins (or sites occupied by adsorbate atoms), small dots represent “down” spins (or empty lattice sites). The unit cells corresponding to the “structure” entries in Table 2 are shown. The additional hexagonal unit cells displayed for the (1×3) and (3×3) configurations may be used to prove the equality of all two-spin correlation functions for these structures (see text)

configurations are well-known (see references quoted in the introduction), but the question of uniqueness was not definitely settled up to now.

For the two configurations 4a and 4b *all* two-spin correlation functions are equal. This is most easily seen by choosing hexagonal unit cells for both configurations (see Fig. 1). Then, by translation invariance, c_1 and c_2 turn out to be the only independent two-spin correlation functions. This argument does not hold for three-spin correlation functions, and indeed, the correlation function corresponding to the corners of a nearest-neighbour triangle yields different values for the two configurations. (The values of this correlation function are the entries in the “ c_A ” column of Table 2. c_A is bounded by ± 1 , as are c_1 and c_2 .) It should be noted that a “fine-grained mixture” of the two configurations does *not* correspond to $m=1/3$, $c_1=1/9$ and $c_2=-1/3$, because these values imply that every next-nearest-neighbour triangle contains exactly one “down” spin and this condition would be violated at any interface between different domains. Thus, these two degenerate configurations are not arbitrarily miscible. Due to the equality of all two-spin correlation functions the degeneracy of the two configura-

tions cannot be removed by any (isotropic) two-spin interaction. (An additional two-spin interaction may, however, lead to the appearance of totally new ground state configurations.) The degeneracy can be removed, e.g. by an interaction between the three spins at the corners of a nearest-neighbour triangle, as the appropriate correlation function yields different values for the two configurations.

III. Effects of a Three-Spin-Interaction

We now supplement the Hamiltonian (II.1) by a term

$$H_A = -4J_A \sum_A \sigma_i \sigma_j \sigma_k = -NJ_A c_A \quad (\text{III.1})$$

representing an interaction between three spins at the vertices i, j, k of an “elementary triangle” of nearest-neighbour bonds. The summation is performed over all $2N$ elementary triangles of an N -site lattice. c_A denotes the corresponding three-spin correlation bounded by ± 1 , as already mentioned in the preceding section. Note that c_A changes sign under spin reversal, as does m . The model described by the Hamiltonian (III.1) alone was solved exactly by Baxter and Wu [19].

In the lattice gas model, a three-particle interaction may be described by adding the term

$$H_{A,lg} = \Gamma_A \sum_A n_i n_j n_k \quad (\text{III.2})$$

to the grand canonical lattice gas Hamiltonian (II.2). In this case, the correspondences between coupling parameters of Ising and lattice gas Hamiltonians are given by the following generalization of (II.3):

$$\begin{aligned} B &\leftrightarrow \frac{\varepsilon + \mu}{2} - \frac{3}{2}(\Gamma_1 + \Gamma_2) - 3\Gamma_A, \\ J_1 &\leftrightarrow -\frac{3}{4}\Gamma_1 - \frac{3}{2}\Gamma_A, \\ J_2 &\leftrightarrow -\frac{3}{4}\Gamma_2, \quad J_A \leftrightarrow -\frac{1}{4}\Gamma_A. \end{aligned} \quad (\text{III.3})$$

(Note that the n -particle interactions of the lattice gas influence “lower-order” interactions of the Ising model.)

In analogy to Sect. II we shall now try to determine the four-dimensional convex set of all points (m, c_1, c_2, c_A) corresponding to possible spin configurations of the system. We observe that the ground state configurations for $J_A=0$ derived in the preceding section form a subset of the possible ground state configurations of the system for nonvanishing J_A , as they are already *uniquely* determined by the

constraints on m , c_1 , and c_2 . Thus the vectors (m, c_1, c_2, c_4) corresponding to these states span a four-dimensional simplex which is certainly *smaller* than (and included in) the desired set; furthermore all corners of the smaller set are also corners of the larger set. On the other hand, the inequalities collected in Table 1 do not restrict the values of c_4 and thus define a four-dimensional simplex which is certainly *larger* than the desired set (and includes it). In the following, we shall approach the desired set by expanding the simplex spanned by the known configurations as well as by proving more restrictive inequalities.

In order to estimate the influence of a three-spin interaction on the number of possible ground state configurations, one may study a simpler system, for example the case $J_2=0$. It turns out that in this case the introduction of a three-spin interaction does not bring about any new configurations. The same holds true also for the case $J_1=0$ and – mutatis mutandis – for a one-dimensional system. This makes us hope that the additional term (III.1) will not make the number of possible ground states intractably large. (It is, however, not certain that the number of ground state configurations remains finite; Kanamori [9] has reported an infinite sequence of possible ground state structures for an Ising model on a honeycomb lattice with interactions up to third neighbours.)

Some inequalities involving the triangle correlation c_4 may be derived by the methods introduced in the preceding section. Considering, for example, four spins $\sigma_1, \dots, \sigma_4$ situated at the vertices of a rhomb formed by two elementary triangles, such that σ_2 and σ_3 are nearest neighbours and σ_1 and σ_4 are next-nearest neighbours, one may define

$$c_4 = \frac{1}{N} \sum_i (4\sigma_1 \sigma_2 \sigma_3 + 4\sigma_2 \sigma_3 \sigma_4), \quad (\text{III.4a})$$

$$3m + c_4 = \frac{4}{N} \sum_i \left(\frac{\sigma_1 + \sigma_2}{2} + \frac{\sigma_3}{2} + 2\sigma_1 \sigma_2 \sigma_3 \right), \quad (\text{III.4b})$$

$$m - c_4 = \frac{2}{N} \sum_i (\sigma_1 - 4\sigma_1 \sigma_2 \sigma_3). \quad (\text{III.4c})$$

(i denotes the position of one of the spins, say of σ_1 .) Then, using the triangle inequality and (II.6a), one obtains the inequalities

$$-1 \leq c_2 - 2|c_4|, \quad (\text{III.5a})$$

$$-1 \leq -|3m + c_4| + 3c_1, \quad (\text{III.5b})$$

$$-1 \leq -|m - c_4| - c_1. \quad (\text{III.5c})$$

It is obvious from these examples that there are many possibilities of constructing inequalities, most of which however, turn out to be useless.

In order to avoid a tedious trial and error procedure, a computer algorithm was developed which generates a set of inequalities from the set of all possible configurations of a cluster containing only a few spins. For such a cluster, one may define quantities analogous to m , c_1 , c_2 , and c_4 by assigning arbitrary (but fixed) weights to the points, bonds, and triangles of the cluster. The finite set of points in four-dimensional space which is generated by calculating the above-mentioned quantities for all possible spin configurations of the cluster then spans a simplex representing a set of true inequalities. The shape of the cluster and the weights may be varied in order to optimize the inequalities. A more detailed account of this method may be found in [28].

There is a slight similarity between the present algorithm and the “linear programming” procedure suggested by Allen and Cahn [29] to determine the ground state structures of bcc and fcc ordered binary alloys. The method of Allen and Cahn, however, is more ambitious than ours, as these authors directly determine the ground state configurations of an infinite lattice from the configurations of a cluster, whereas our method is more flexible. We note in passing that we have tested our method for the square lattice Ising model with interactions up to third-nearest neighbours. It turned out to be quite easy to derive the full set of inequalities necessary to determine the ground states, a task which is rather arduous to perform analytically [6–8].

Using the method sketched above, we were able to derive two more useful inequalities (among several others), namely

$$-1 \leq -|m - c_4| \pm 2c_1 + c_2, \quad (\text{III.6a})$$

$$-1 \leq -\frac{1}{2}|m \pm 3c_4| \pm \frac{3}{2}c_1 + \frac{3}{2}c_2. \quad (\text{III.6b})$$

(Where the double “ \pm ” is to be interpreted as “+ , + or – , –”.) A cluster of seven spins (a central spin and its nearest neighbours) was used in both cases. To derive (III.6a), the central spin was not taken into account for the magnetization; all other spins, bonds, and triangles were given equal weights. To derive (III.6b), only the central spin was counted for the magnetization and only the bonds between the outer spins were used to calculate c_1 .

The inequalities (III.5) and (III.6) serve to reduce the size of the “outer simplex” defined by the known inequalities. In order to enlarge the “inner simplex” spanned by the configurations of Sect. II we performed small-scale Monte Carlo simulations giving useful hints for the construction of candidate ground state configurations. We found four new configurations which are listed in Table 3 and depicted in Fig. 2.

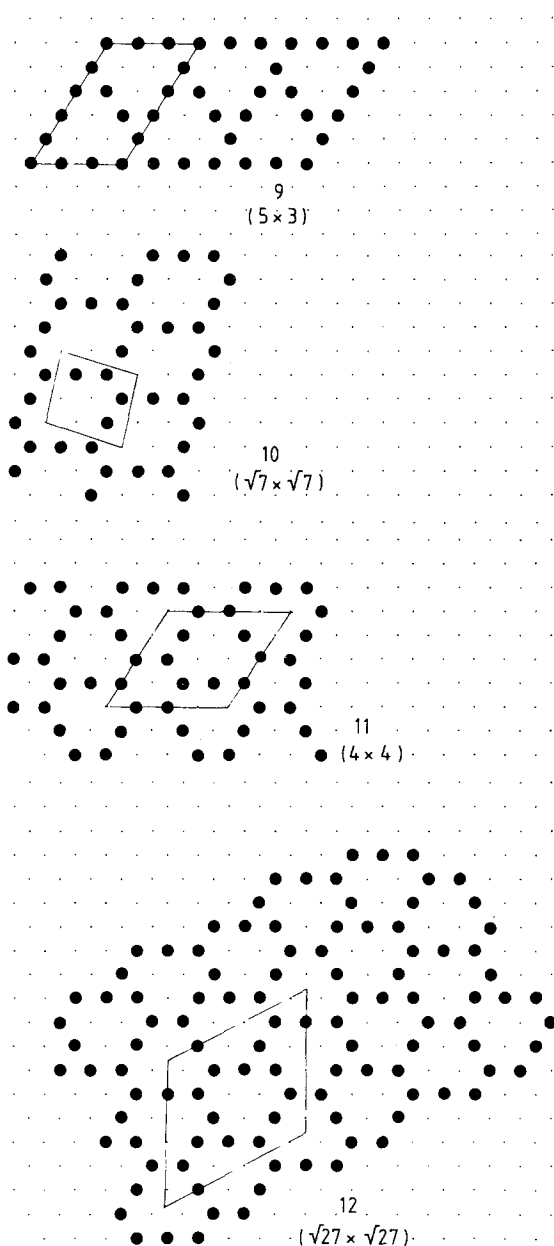


Fig. 2. Lattice configurations corresponding to the states listed in Table 3. Big dots correspond to “up” spins (occupied sites). Unit cells are shown

Table 3. Additional ground states of the Ising model (III.1), as characterized by magnetization, two- and three-spin correlations, and superlattice unit cells. 10–12 are only tentative

Corner No.	m	c_1	c_2	c_4	Structure
9	1/5	-1/15	-1/3	-1/3	5 × 3
10	0	-1/6	0	1/2	$\sqrt{7} \times \sqrt{7}$
11	1/8	-1/4	1/4	-5/8	4 × 4
12	1/9	-5/27	-1/27	-13/27	$\sqrt{27} \times \sqrt{27}$

Due to the method of construction, we do not know whether there is a unique correspondence between the parameter values of Table 3 and the structures of Fig. 2. We do not even know whether corners 10, 11, and 12 are genuine ground states, as there is still a difference between the outer and inner simplices which we were not able to remove.

The “outer simplex” is described by inequalities 3, 6, 8, 9, 10 from Table 1 (together with their spin-reversed counterparts), and inequalities (III.5) and (III.6). This simplex possesses the corners 1 through 6, 9, (cf. Tables 2 and 3) and an additional corner with the parameter values

$$(m, c_1, c_2, c_4) = \frac{1}{13}(1, -3, 1, -7) \tag{III.7}$$

(plus the spin-reversed counterparts of the points mentioned). We could not find a configuration corresponding to (III.7). (The numerical values suggest that a suitable configuration might have a $\sqrt{13} \times \sqrt{13}$ structure, however, there is no $\sqrt{13} \times \sqrt{13}$ configuration fulfilling (III.7).)

The “inner simplex”, on the other hand, comprises the corners 1 through 6 and 9 through 12. It is described by the same set of inequalities as the “outer simplex”, plus the additional inequality

$$-1 \leq -\frac{5}{11}|m + 3c_4| + \frac{21}{11}c_1 + \frac{12}{11}c_2. \tag{III.8}$$

which we could not prove. We were able, however, to prove (III.8) with the left hand side replaced by $-151/143$, using the same “hexagon” cluster as for the proof of (III.6), with optimized weights. Incidentally, $-151/143$ is the number which results if the values (III.7) are inserted into (III.8).

The inequality (III.8) (with $(m + 3c) \leq 0$) is fulfilled as an equality by the points 6, $\bar{10}$, 11, and 12. (The overbar denotes inversion of all spins, as compared to the configurations listed in the tables and displayed in the figures.) These points, together with (III.7), obviously span a four-dimensional “pentahedron” which makes up half of the difference between the inner and outer simplices. (The other half is spanned by the spin-reversed versions of these points.) The four-volume of one such pentahedron is approximately $1.3 \cdot 10^{-5}$, compared to a total volume of 0.9433 of the whole simplex, so we may conclude that there is not much room for additional ground state configurations to hide in.

IV. Ground State Phase Diagrams

From the ground state configurations derived in the two preceding sections one may easily construct “ground state phase diagrams” by determining

which one of these states yields the lowest energy for given values of the coupling parameters. The set of points in coupling parameter space for which a given configuration is the ground state may be called the stability region of this phase. As discussed in Sect. II, the parameter vectors (m, c_1, c_2, c_d) of the ground states are *corners* of the simplex of possible values of this vector. Therefore the stability regions in the "dual space" of (B, J_1, J_2, J_d) vectors are *convex*. The faces of the simplex, which are defined by the inequalities, obviously correspond to points of multi-phase coexistence in coupling parameter space. If, for instance, some configurations fulfill the inequality

$$-1 \leq a_1 m + a_2 c_1 + a_3 c_2 + a_4 c_d \quad (\text{IV.1})$$

as an equality, then at the point

$$(B, J_d, J_2, J_1) = -|\varepsilon|(a_1, a_2, a_3, a_4) \quad (\text{IV.2})$$

in coupling parameter space all these configurations have the energy $-|\varepsilon|$ (per spin) and no other configuration has a lower energy. This property is helpful in locating interesting regions in coupling parameter space.

For the model (II.1) (without three-spin coupling) we have the coupling parameters B, J_1 , and J_2 . Obviously it suffices to consider the parameters $J_1/|B|$ and $J_2/|B|$; the sign of B only distinguishes between the configurations of Fig. 1 and their "spin-inverted" counterparts. The situation studied by Wannier [1], i.e. $J_1 < 0, B = J_2 = 0$, corresponds to a point at negative infinity on the $J_1/|B|$ axis of Fig. 3, where the configurations 3, $\bar{3}$, and 6 (the $c_1 = -1/3$ configurations) coexist. (The overbar again denotes spin inversion.) For $J_1 = 0$ and $B \rightarrow 0$ we observe either coexistence of all structures with $c_2 = 1$ (for positive J_2) or of all structures with $c_2 = -1/3$ (for negative J_2). The configurations with nontrivial unit cells are of course all degenerate due to symmetry, for example the $\sqrt{3} \times \sqrt{3}$ configuration has a threefold degeneracy. Thus the stability region of this phase really is a region of coexistence between three degenerate phases with domain walls separating the phases in space. (Domain walls in $\sqrt{3} \times \sqrt{3}$ phases have been frequently discussed in connection with ordering phenomena in layers of krypton and xenon adsorbed on graphite; see [4] and references cited there.) From Fig. 3 one may derive the corresponding phase diagram of the lattice gas model (II.2). As the reversal of the field B in the Ising model corresponds to a more complicated operation in terms of the lattice gas parameters $(\varepsilon + \mu), \Gamma_1$, and Γ_2 (cf. (II.3)), it is useful to draw two "phase diagrams" for the lattice

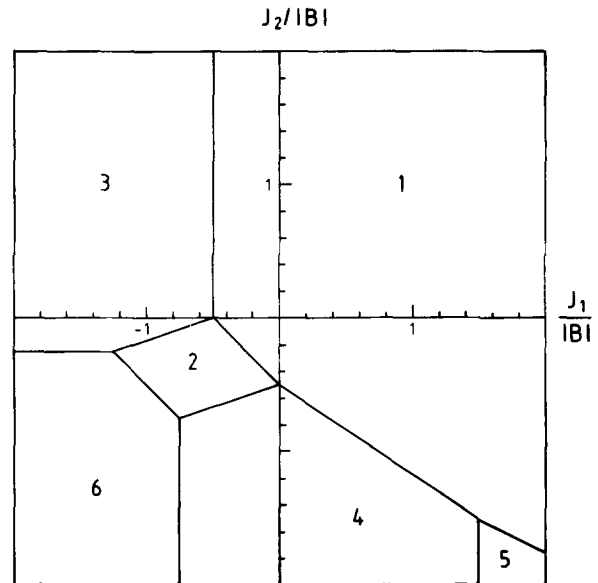


Fig. 3. "Ground state phase diagram" of the Ising model (II.1). The numbers in the different regions denote either the configurations of Fig. 1 or their "spin-inverted versions", according to the sign of the external field B

gas model, distinguishing the cases $\Gamma_1 > 0$ and $\Gamma_1 < 0$ (Figs. 4a and 4b).

In an adsorption experiment, the chemical potential μ may be varied by changing the adsorbate gas pressure. Thus one may study a section of the lattice gas phase diagram along a line parallel to the $(\varepsilon + \mu)$ -axis. It is important to note in this context that the lattice gas model allows for two kinds of transition, one of which simply consists in adding (or removing) adsorbate particles (e.g. the transition from an empty lattice to any other configuration), whereas the other sort of transition involves a complete reordering of the structure, enforced by a change in superlattice symmetry (e.g. the transition between states 2 and 4). The nature of the transitions occurring at finite temperature may be studied by real or Monte Carlo experiments; for example a pronounced hysteresis effect vanishing above a certain temperature has been observed [13] in a Monte Carlo simulation studying the transition between phases 3 and $\bar{3}$. The actual behaviour in a real adsorption experiment of course depends on details which have not been considered here.

We wish to stress that the method described above yields *all possible* ground state configurations, assuming interactions between nearest and next-nearest neighbours only. The occurrence of any other adsorbate superlattice on a substrate with a triangular lattice of adsorption sites must be considered an indication of more complicated (e.g. long range, anisotropic, or many-body) interactions.

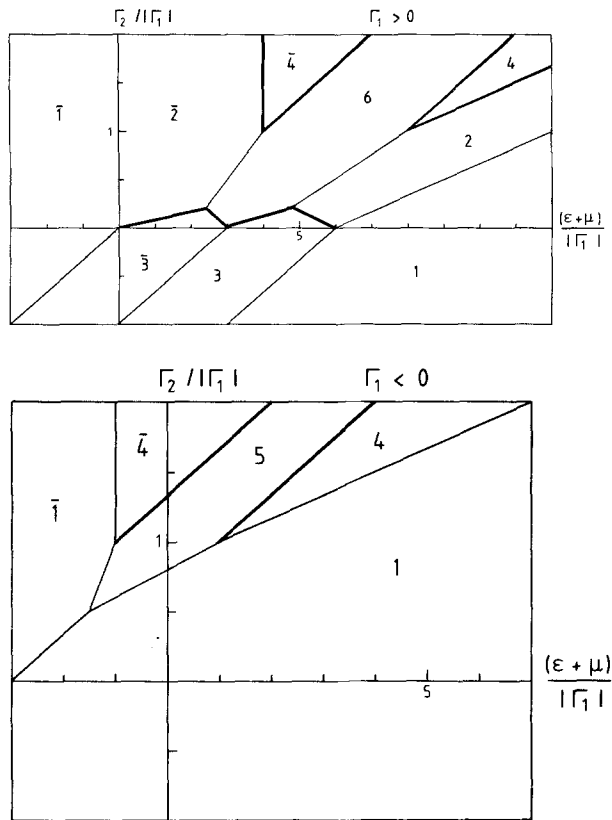


Fig. 4a and b. “Ground state phase diagrams” for the lattice gas model (II.2) with repulsive (a) or attractive (b) nearest-neighbour interactions. The numbers refer to the configurations of Fig. 1, the overbar denotes the replacement of occupied sites by empty sites and vice versa. Thin lines denote transitions without reordering, heavy lines denote reordering transitions

To illustrate the behaviour of the system for non-vanishing three-spin coupling we display two phase diagrams for different values of J_Δ/B in Figs. 5 and 6. Due to the incompleteness of our solution (see Sect. II) there is some uncertainty in these phase diagrams. However, this concerns only the configurations fulfilling the “uncertain inequality” (III.8) as an equality, i.e., configurations 6, 10, 11, and 12 (plus their spin-reversed counterparts). The stability regions of these configurations are the only ones which might be affected if a configuration violating (III.8) were found. In this case the stability regions of the abovementioned points would shrink (or even vanish), while the stability regions of the new configuration would appear. The stability regions of all other configurations are completely determined and would not be affected by the appearance of a new corner of the simplex.

In Fig. 6 a point of coexistence between five different ground state phases (namely 1, $\bar{3}$, 4a, 10, $\bar{11}$) is visible. The coordinates of this point (which are only defined up to a factor) may be fixed to (B, J_1, J_2, J_Δ)

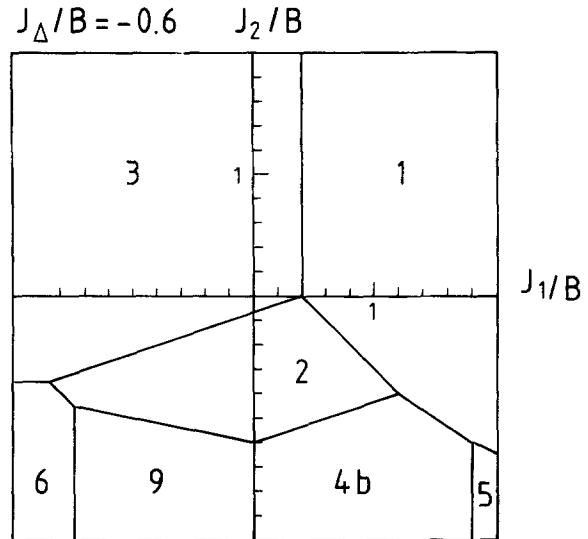


Fig. 5. Section through the “ground state phase diagram” of the Ising model (III.1) at $J_\Delta/B = -0.6$ ($B > 0$). The numbers in the various regions correspond to those used in Figs. 1 and 2

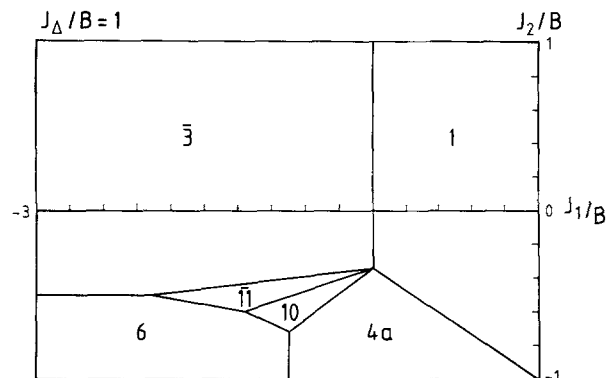


Fig. 6. Section through the “ground state phase diagram” of the Ising model (III.1) at $J_\Delta/B = 1$ ($B > 0$). The numbers in the various regions correspond to those used in Figs. 1 and 2; the overbar denotes inversion of all spins, as compared to Figs. 1 and 2. The point of coexistence between five phases occurring here actually is only one point of a whole line on which these phases coexist. The stability region of phase 5, which is visible on the lower right of Figs. 3 and 5, lies outside the frame of this figure

$= 1/2 (3, -3, -1, 3)$. This point of coexistence does not correspond to one face of the four-dimensional simplex of configurations, but to an edge between two faces. These two faces correspond to the points

$$(B, J_1, J_2, J_\Delta) = (0, 0, 1, -2) \quad \text{and} \quad (-3, 3, 0, -1)$$

(see inequalities (III.5a, b)). In addition to the five ground state phases mentioned above, we find at the first of these points the configurations $\bar{2}$, $\bar{9}$, and $\bar{12}$, and at the second one the configurations 2, 3 and 6.

For the case $J_2 = 0$ our ground state phase diagrams agree with those derived in [18] by real space

renormalization group methods (see Figs. 13 and 18 of [18]), showing the configurations 1, $\bar{1}$, 3, and $\bar{3}$, separated by first-order and higher-order boundaries. The higher-order boundaries of [18] turn out to be lines of coexistence of *three* phases, with one of the phases 2, $\bar{2}$, or 6 also present. At the “triple points” in the case of negative J_1 , ground states of the types 4a, 10, and 11 show up too. These “zero-measure stability regions” will either vanish completely or become finite in case of slight deviations from $J_2=0$.

Ground state phase diagrams in the lattice gas variables $(\varepsilon+\mu)$, I_1 , I_2 , and I_d may be easily obtained by means of the transformation (III.3); however, we shall not present any further phase diagrams for reasons of space. For comparison to experiments on adsorbed layers, it would be interesting to replace $(\varepsilon+\mu)$ by its thermodynamically conjugate variable, the surface density (coverage). In order to perform this transformation, it is essential to know whether the transitions between different “phases” are of “first order” or “continuous”. This question may be attacked by studying the energy of an interface between the two phases in question: if the interface energy is positive, the system will try to minimize interface length by forming spatially well-separated domains and the transition will be one of “first order”; if the interface energy happens to vanish, the two phases may mix up freely and a “continuous” transition may take place. (For finite temperature, interface entropy of course becomes important.)

To determine the energy of an interface between two given phases, one may check whether all those local constraints on the spin configuration are satisfied which are implied by the inequalities fulfilled as equalities at coexistence. If it is possible to build up an interface while satisfying all these constraints, the interface energy vanishes. This method of determining the nature of transitions between different ground state configurations was used successfully for an extended Hubbard model in the atomic limit [28]. However, due to the relatively large number of different ground state configurations of the present model, and due to the rather complicated nature of the inequalities by which they are determined, we refrain from carrying through a similar discussion here.

We are grateful to Johannes Pollmann for some helpful discussions.

References

1. Wannier, G.H.: Phys. Rev. **79**, 357 (1950)
2. Houtappel, R.M.F.: Physica **16**, 425 (1950)
3. Dash, J.G.: Films on solid surfaces. New York: Academic Press 1975
4. Birgeneau, R.J., Horn, P.M.: Science (to be published)
5. Dresselhaus, M.S.: Festkörperprobleme. Adv. Solid State Phys. **XXV**, 21 (1985)
6. Kaburagi, M.: J. Phys. Soc. Jpn. **44**, 54 (1978)
7. Brandt, U.: Z. Phys. B - Condensed Matter **53**, 283 (1983)
8. Kanamori, J., Kaburagi, M.: J. Phys. Soc. Jpn. **52**, 4184 (1983)
9. Kanamori, J.: J. Phys. Soc. Jpn. **53**, 250 (1984)
10. See Somorjai, G.A., Hove, M.A. van: Adsorbed monolayers on solid surfaces. In: Structure and bonding. Vol. 38. Berlin, Heidelberg, New York: Springer Verlag 1979 for an impressive (although meanwhile probably outdated) collection of structures
11. Metcalf, B.D.: Phys. Lett. **A45**, 1 (1974)
12. Mihura, B., Landau, D.P.: Phys. Rev. Lett. **38**, 977 (1977)
13. Landau, D.P.: Phys. Rev. B **27**, 5604 (1983)
14. Campbell, C.E., Schick, M.: Phys. Rev. A **5**, 1919 (1972)
15. Kaburagi, M., Tonegawa, T., Kanamori, J.: J. Phys. Soc. Jpn. **51**, 3857 (1982)
16. Slotte, P.A., Hemmer, P.C.: J. Phys. C: Solid State Phys. **17**, 4645 (1984)
17. Müller-Hartmann, E., Zittartz, J.: Z. Phys. B **27**, 261 (1977)
18. Schick, M., Walker, J.S., Wortis, M.: Phys. Rev. B **16**, 2205 (1977)
19. Baxter, R.J., Wu, F.Y.: Phys. Rev. Lett. **31**, 1294 (1973); Aust. J. Phys. **27**, 357 (1974)
20. Berker, A.N., Ostlund, S., Putnam, F.A.: Phys. Rev. B **17**, 3650 (1978)
21. Metcalf, B.D.: Phys. Lett. A **46**, 325 (1974)
22. Kaburagi, M., Kanamori, J.: Jpn. J. Appl. Phys. Suppl. **2**, Part 2, 145 (1974)
23. Kaburagi, M., Kanamori, J.: Prog. Theor. Phys. **54**, 30 (1975)
24. Kanamori, J.: Ann. Phys. (Paris) **10**, 43 (1985)
25. Kudo, T., Katsura, S.: Prog. Theor. Phys. **56**, 435 (1976)
26. Tanaka, Y., Uryû, N.: J. Phys. Soc. Jpn. **39**, 825 (1975); Prog. Theor. Phys. **55**, 1356 (1976)
27. Kaburagi, M., Kanamori, J.: J. Phys. Soc. Jpn. **44**, 718 (1978)
28. Brandt, U., Stolze, J.: Z. Phys. B - Condensed Matter **62**, 433 (1986)
29. Allen, S.M., Cahn, J.W.: Acta Metall. **20**, 423 (1972)

U. Brandt
J. Stolze
Institut für Physik
Universität Dortmund
Postfach 500500
D-4600 Dortmund 50
Federal Republic of Germany